Title

Head-to-Tail Intramolecular Interaction of Herpes Simplex Virus Type 1 Regulatory Protein ICP27 Is Important for Its Interaction with Cellular mRNA Export Receptor TAP/NXF1

Journal

mBio, 1(5)

ISSN

2150-7511

Authors

Hernandez, Felicia P

Sandri-Goldin, Rozanne M

Publication Date

2010-11-09

DOI

10.1128/mBio.00268-10

Head-to-Tail Intramolecular Interaction of Herpes Simplex Virus Type 1 Regulatory Protein ICP27 Is Important for Its Interaction with Cellular mRNA Export Receptor TAP/NXF1

Felicia P. Hernandez* and Rozanne M. Sandri-Goldin

Department of Microbiology and Molecular Genetics, School of Medicine, University of California, Irvine, California, USA

* Present address: Scripps Research Institute, 10550 North Torrey Pines Road, La Jolla, California, USA.

ABSTRACT **Herpes simplex virus type 1 (HSV-1) protein ICP27 has many important functions during infection that are achieved through interactions with a number of cellular proteins. In its role as a viral RNA export protein, ICP27 interacts with TAP/NXF1, the cellular mRNA export receptor, and both the N and C termini of ICP27 must be intact for this interaction to take place. Here we show by bimolecular fluorescence complementation (BiFC) that ICP27 interacts directly with TAP/NXF1 during infection, and this interaction failed to occur with an ICP27 mutant bearing substitutions of serines for cysteines at positions 483 and 488 in the C-terminal zinc finger. Recently, we showed that ICP27 undergoes a head-to-tail intramolecular interaction, which could make the N- and C-terminal regions accessible for binding to TAP/NXF1. To determine the importance of intramolecular association of ICP27 to its interaction with TAP/NXF1, we performed BiFC-based fluorescence resonance energy transfer (FRET) by acceptor photobleaching. BiFC-based FRET showed that the interaction between ICP27 and TAP/NXF1 occurred in living cells upon head-to-tail intramolecular association of ICP27, further establishing that TAP/NXF1 interacts with both the N and C termini of ICP27.**

IMPORTANCE **ICP27 is a key regulatory protein during herpes simplex virus type 1 (HSV-1) infection. ICP27 interacts with a number of cellular proteins, and an important question asks how these interactions are regulated during infection. We showed previously that ICP27 undergoes a head-to-tail intramolecular interaction, and here we show that the cellular mRNA export receptor protein TAP/NXF1 interacts with ICP27 after its head-to-tail association. Several proteins that interact with ICP27 require that the N and C termini of ICP27 be intact. These results demonstrate that the head-to-tail interaction of ICP27 may regulate some of its protein interactions perhaps through alternating between open and closed configurations.**

Received 12 October 2010 **Accepted** 15 October 2010 **Published** 9 November 2010

Citation Hernandez, F. P., and R. M. Sandri-Goldin. 2010. Head-to-tail intramolecular interaction of herpes simplex virus type 1 regulatory protein ICP27 is important for its interaction with cellular mRNA export receptor TAP/NXF1. mBio 1(5):e00268-10. doi:10.1128/mBio.00268-10.

Editor Michael Imperiale, University of Michigan Medical School

Address correspondence to Rozanne M. Sandri-Goldin, rmsandri@uci.edu.

ICP27 is an essential regulatory protein that plays many different roles during herpes simplex virus type 1 (HSV-1) infection. ICP27 interacts with a number of cellular proteins, and these include proteins that are involved in pre-mRNA splicing (1, 2), mRNA export (3, 4), nuclear protein quality control (5), type I interferon signaling (6), apoptosis (7, 8), and translation initiation (9, 10). ICP27-protein interactions have been demonstrated in yeast two-hybrid screens, *in vitro* binding assays, coimmunoprecipitation experiments, and colocalization studies. The regions of ICP27 that are required for interaction with various binding partners have been mapped by mutational analysis (11). Both the N-terminal leucine-rich region and the C-terminal zinc finger region of ICP27 must be intact for its interaction with RNA polymerase II (12), mRNA export receptor TAP/NXF1 (3), and heat shock cognate protein Hsc70 (5). How the different interactions of ICP27 are regulated throughout infection is not well understood. ICP27 is posttranslationally modified by phosphorylation (13) and arginine methylation (14, 15), and we have shown that phosphorylation and arginine methylation can regulate some of ICP27's protein interactions (15–18).

A number of cellular proteins have been shown to undergo interactions of their N and C termini in a reversible manner that regulates their protein interactions. These include scaffold proteins such as zyxin (19), myosin VIIA (20), PDZK1 (21), and talin (22), as well as the motor protein kinesin (23, 24) and Raf kinase (25). Head-to-tail intramolecular interaction alters protein conformation and thus may serve as a mechanism for regulating protein interactions. For example, HSV-1 glycoprotein D (gD) exists in two conformations. In the closed conformation, the C terminus and the N terminus interact. When gD encounters its cellular receptor, the N and C termini are released from reciprocal interactions in an open conformation, which triggers fusion (26). We have shown that ICP27 undergoes head-to-tail intramolecular interaction (27) using bimolecular fluorescence complementation (BiFC) assays (28, 29) and fluorescence resonance energy transfer (FRET) by acceptor photobleaching (30). We postulate that

ICP27 may undergo intramolecular head-to-tail association to interact with those proteins that require its intact N and C termini.

ICP27 interacts with cellular mRNA export receptor TAP/NXF1 in its role as a viral RNA export protein (3, 4). Interaction with TAP/NXF1 is absolutely required for export of ICP27 to the cytoplasm (3, 5, 31) and for export of viral RNA (31, 32). ICP27 also interacts with Hsc70 and is required for Hsc70 recruitment into nuclear foci called VICE (virus-induced chaperone-enriched) domains, which appear to play a role in nuclear protein quality control during HSV-1 infection (5, 33, 34). ICP27 has been shown to coimmunoprecipitate and colocalize with TAP/NFX1 and Hsc70 during infection (3–5). In this report, we used BiFC assays to demonstrate that ICP27 associates with TAP/NXF1 and Hsc70 on a nanometer scale, and mutations within ICP27's C-terminal zinc finger prevented functional association. Further, we show that interaction between TAP/NXF1 and ICP27 can be detected only by FRET analysis upon the intramolecular head-to-tail association of ICP27.

RESULTS

ICP27 interacts with TAP/NXF1 directly. ICP27 colocalizes with TAP/NXF1 during HSV-1 infection (Fig. 1A), and this association requires that the N and C termini of ICP27 are intact (3). Functional association with TAP/NXF1 is required for ICP27 export to the cytoplasm (3, 4). Mutant ICP27-C483,488S, in which cysteine residues 483 and 488 in the C-terminal zinc finger were substituted with serine residues, did not colocalize with TAP/NXF1, and mutant ICP27 was exclusively nuclear, even at late times after infection (Fig. 1A). To verify that ICP27 and TAP/NXF1 physically interact, we performed BiFC analysis. The N-terminal half of the yellow fluorescent protein Venus (35) was fused in frame to the N terminus of TAP/NXF1, and the C-terminal half of Venus was fused to the C terminus of ICP27. If two proteins come into close, nanometer-scale contact, the two halves of Venus come together and renature, and fluorescence will occur (29, 36, 37). As a positive control, we used NC-Venus-ICP27, in which the N- and C-terminal halves of Venus are fused to the N and C termini of ICP27 (Fig. 1B), because we have shown that ICP27 undergoes a head-to-tail intramolecular interaction (27). Venus fluorescence was clearly seen with N-Venus–TAP/NXF1 and ICP27–C-Venus, but fluorescence was not detected with N-Venus–TAP/NXF1 and ICP27-C483,488S–C-Venus (Fig. 1C and D). These results indicate that TAP/NXF1 and ICP27 interact on a nanometer scale and that perturbation of the C-terminal zinc finger prevents the interaction. We reported previously that NC-Venus-ICP27-C483,488S did not undergo intramolecular interaction, indicating that alteration of the zinc finger interferes with ICP27's protein interactions (27).

To demonstrate that the lack of fluorescence with ICP27-C483,488S–C-Venus was not due to poor expression, we performed Western blot analysis with cells that were transfected with the ICP27-Venus fusion constructs and N-Venus–TAP/NXF1. Twenty-four hours later, transfected cells were infected with 27-LacZ to induce ICP27 expression by VP16, because all the ICP27 constructs are under the control of the native ICP27 promoter. Cells were harvested 8 h later. N-Venus–TAP/NXF1 was expressed to similar levels, and N-Venus–ICP27-C483,488S was expressed at levels about 2-fold higher than those of ICP27–C-Venus (Fig. 2A). Therefore, the lack of Venus fluorescence in the BiFC assay was due to the lack of intermolecular interaction of mutant ICP27 and TAP/NXF1 and not due to poor protein expression. Further, the interaction of ICP27 and TAP/NXF1 in BiFC assays was a functional interaction because ICP27 was detected in the cytoplasm at 6 and 8 h after infection (Fig. 2B).

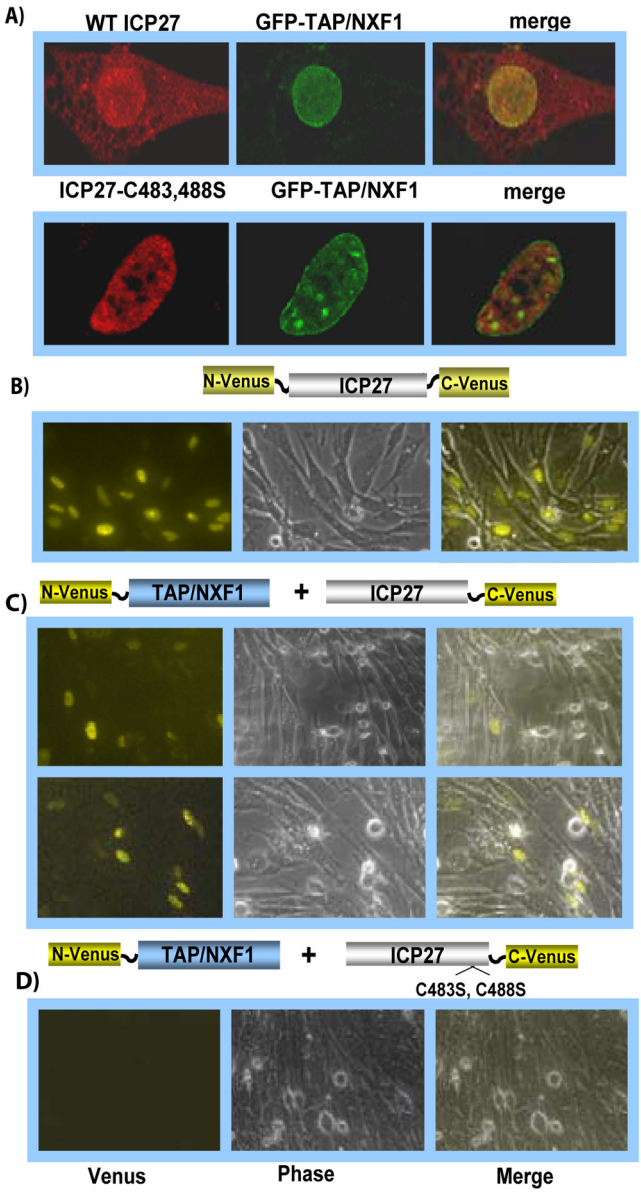

FIG 1 ICP27 interacts directly with TAP/NXF1. (A) RSF were cotransfected with GFP-TAP/NXF1 DNA and with ICP27 constructs carrying wild-type ICP27 or ICP27-C483,488S and were subsequently infected with 27-LacZ for 8 h. Immunofluorescent staining was performed with anti-ICP27 antibody, and GFP fluorescence was viewed directly. (B to D) Cells were transfected with NC-Venus-ICP27 (B) or were cotransfected with N-Venus–TAP/NXF1 and ICP27–C-Venus (C) or with N-Venus–TAP/NXF1 and ICP27-C483,488S–C-Venus (D). Twenty-four hours later, cells were infected with 27-LacZ for 8 h. Cells were viewed directly for Venus fluorescence using a Zeiss LSM 510 Meta confocal microscope at a magnification of ×20.

We wanted to corroborate that ICP27-C483,488S cannot functionally interact with TAP/NXF1 during infection. We constructed an ICP27 viral mutant in which we fused cyan fluorescent protein (CFP) to the N terminus of ICP27-C438,488S. In one-step

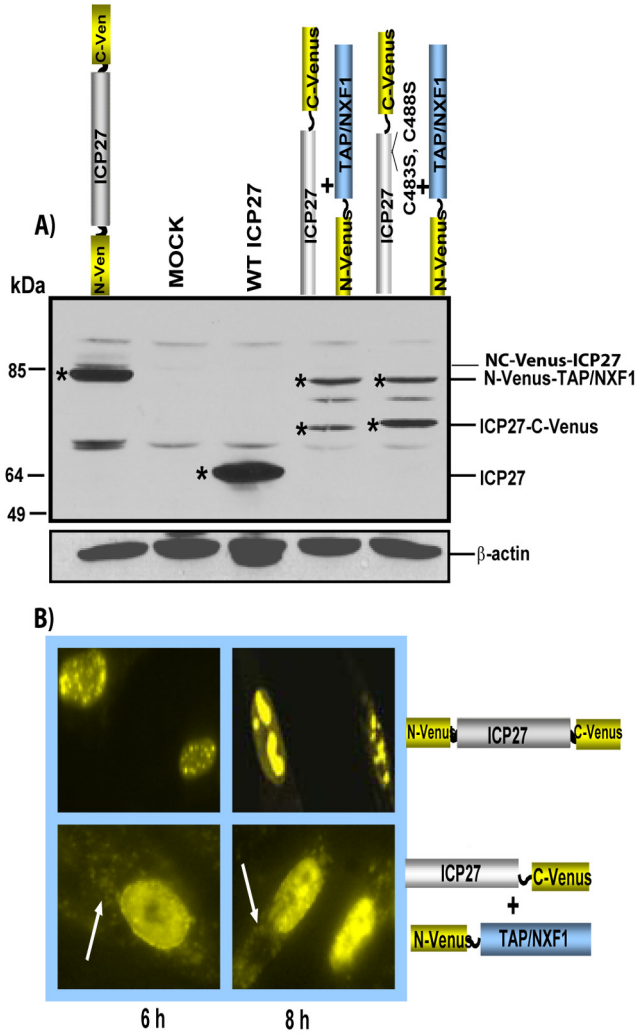

FIG 2 Western blot analysis of TAP/NXF1-Venus and ICP27-Venus fusion proteins. (A) RSF were transfected with plasmid DNA encoding the proteins indicated and infected with 27-LacZ to induce expression of ICP27 constructs. Cells were harvested 8 h after infection, and proteins were fractionated on a 10% SDS-polyacrylamide gel and transferred to nitrocellulose. Membranes were probed with antibodies against GFP, ICP27, and β-actin as described previously (27). Asterisks mark the protein bands. (B) RSF were transfected with NC-Venus-ICP27 or cotransfected with ICP27–C-Venus and N-Venus–TAP/NXF1 and later infected with 27-LacZ for 6 and 8 h, as indicated. Venus fluorescence was viewed directly using a Zeiss LSM 510 Meta confocal microscope at a magnification of ×63. White arrows point to Venus cytoplasmic fluorescence.

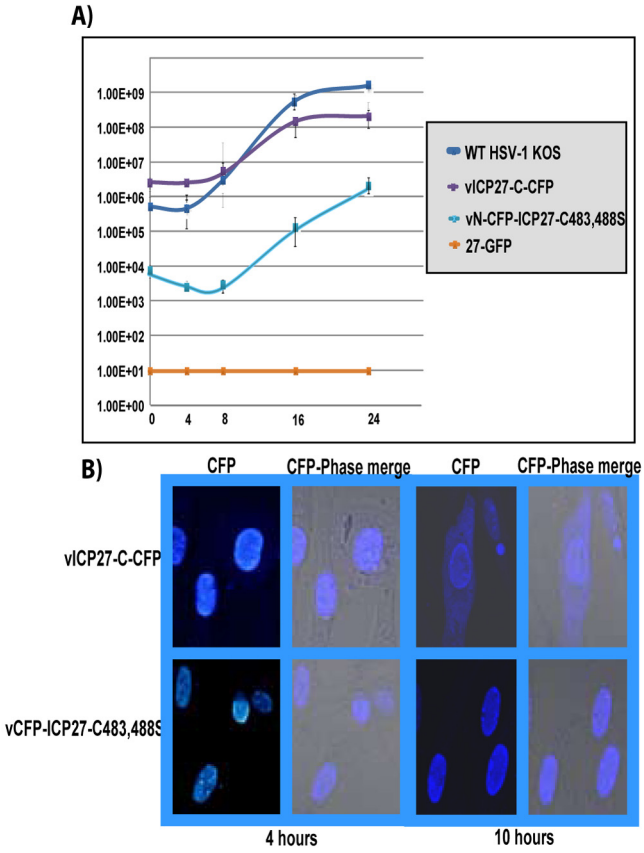

FIG 3 CFP–ICP27-C483,488S is confined to the nucleus during infection. (A) Vero cells were infected with HSV-1 KOS, 27-GFP, vICP27-C–CFP, and vN-CFP–ICP27-C483,488S at an MOI of 1. Experiments were performed in triplicate, and virus was harvested at 0, 4, 8, 16, and 24 h after infection. Plaque assays were performed in duplicate on Vero cells. (B) RSF were infected with vICP27-C–CFP or vN-CFP–ICP27-C483,488S at an MOI of 10 for 4 and 10 h after infection. CFP fluorescence was viewed with a Zeiss LSM 510 Meta confocal microscope at a magnification of ×63.

growth curves, recombinant virus vN-CFP–ICP27-C483,488S yields were reduced by about 3 logs compared to those of wild-type (WT) HSV-1 KOS (Fig. 3A). Another virus, vICP27-C–CFP, in which CFP was fused to the C terminus of ICP27, grew to levels about 5 times lower than those of WT HSV-1 KOS, perhaps because the C-terminal CFP tag might sterically interfere with some of ICP27's interactions. The CFP C-terminal tag did not prevent functional interaction with TAP/NXF1 because ICP27 was clearly seen in the cytoplasm of vICP27-C–CFP-infected cells at 10 h after infection (Fig. 3B), when ICP27 is actively shuttling. In contrast, cytoplasmic CFP fluorescence was not seen in infection with vN-CFP–ICP27-C483,488S (Fig. 3B). We conclude that ICP27 interacts directly with TAP/NXF1 and that the zinc finger is involved in the interaction.

ICP27 interacts directly with Hsc70. ICP27 has been shown to interact with Hsc70 in coimmunoprecipitation and colocalization studies (5), and ICP27 is required for the recruitment of Hsc70 into nuclear foci, or VICE domains, that lie at the periphery of viral replication compartments (5, 33, 34). These VICE domains also contain proteasome components and have been proposed to function in nuclear protein quality control to rid the nucleus of proteins targeted for proteasomal degradation (5, 34). To determine if ICP27 interacts directly with Hsc70, BiFC analysis was performed with N-Venus–Hsc70 and ICP27–C-Venus. Venus fluorescence was seen at 6 and 8 h after infection (Fig. 4). Venus fluorescence was not detected with ICP27-C483,488S–C-Venus at 6 h after infection (Fig. 4A) and was greatly reduced at 8 h compared to that seen with ICP27–C-Venus (Fig. 4B). We verified that all Venus fusion protein constructs were similarly expressed by Western blot analysis (data not shown).

To determine if the BiFC interaction between ICP27 and Hsc70 was functional, as it was for TAP/NXF1, cells were viewed at higher magnification to detect the VICE domains. Immunofluo-

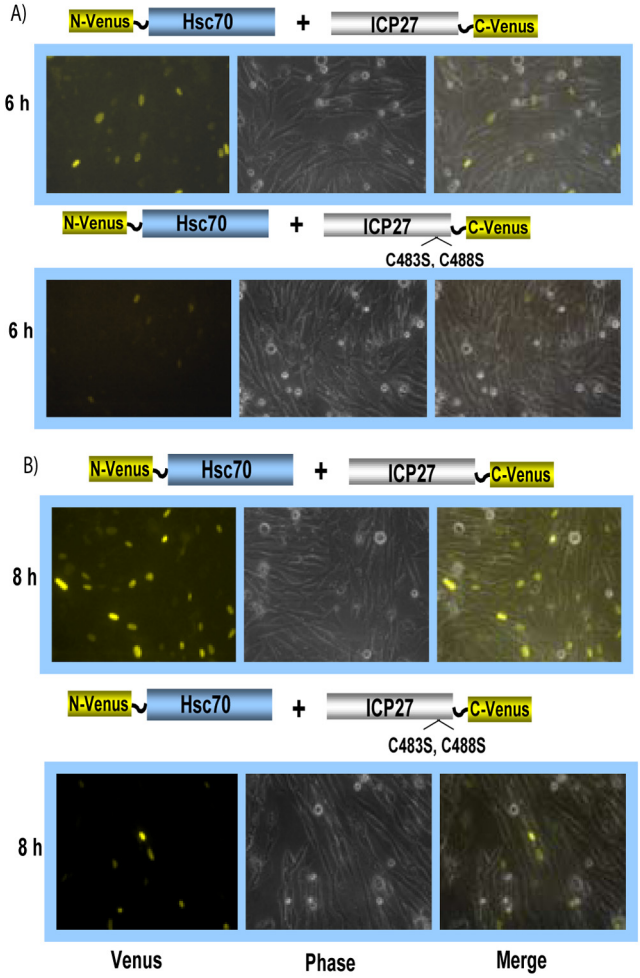

FIG 4 Hsc70 interacts directly with ICP27. RSF were cotransfected with N-Venus–Hsc70 and ICP27–C-Venus or with N-Venus–Hsc70 and ICP27-C483,488S–C-Venus as depicted and were subsequently infected with 27-LacZ for 6 h (A) or 8 h (B). Venus fluorescence was viewed with a Zeiss LSM 510 Meta confocal microscope at a magnification of ×20.

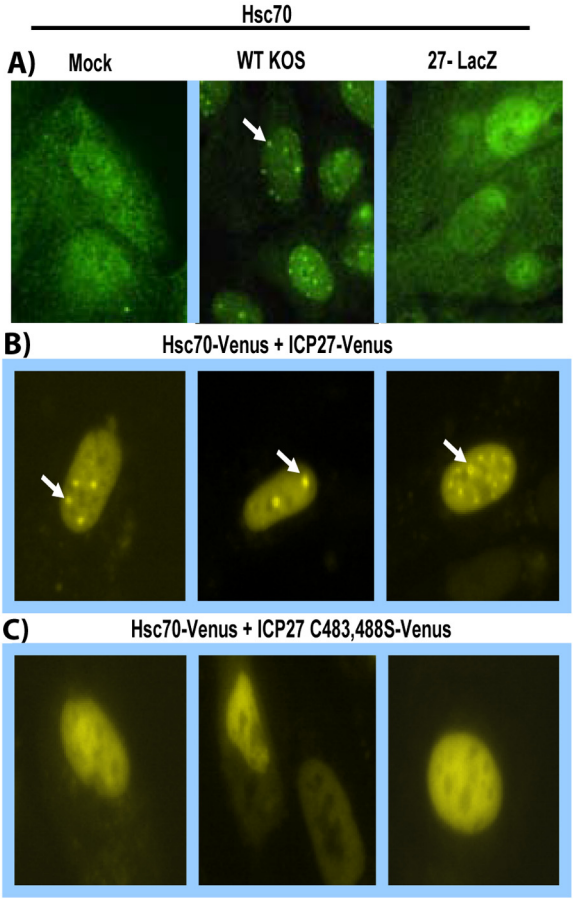

FIG 5 Mutation of the ICP27 zinc finger affects the functional interaction of ICP27 and Hsc70. (A) RSF were either mock infected or infected with HSV-1 KOS or 27-LacZ as indicated for 6 h. Cells were fixed and stained with anti-Hsc70 antibody as described (5). (B, C) RSF were cotransfected with N-Venus–Hsc70 and ICP27–C-Venus (B) or with ICP27-C483,488S–C-Venus (C) as indicated and infected with 27-LacZ. At 8 h after infection, Venus fluorescence was viewed using a Zeiss LSM 510 Meta confocal microscope at a magnification of ×63. White arrows point to Hsc70 nuclear foci.

rescent staining of Hsc70 in mock- and 27-LacZ-infected cells showed a diffuse nuclear and cytoplasmic distribution of Hsc70, as we reported previously (Fig. 5A). In HSV-1 KOS-infected cells, Hsc70 can be seen to be redistributed and concentrated in nuclear foci (Fig. 5A). Nuclear foci were also evident in cells in which BiFC had occurred between Hsc70 and ICP27 (Fig. 5B). Diffuse nuclear fluorescence with some cytoplasmic fluorescence was seen in BiFC between Hsc70 and ICP27-C483,488S (Fig. 5C), indicating that the ICP27 zinc finger mutation affects the functional interaction between ICP27 and Hsc70.

BiFC-based FRET after photobleaching showed that TAP/NXF1 interacts with ICP27 during intramolecular association. We further explored the interaction between TAP/NXF1 and ICP27 using the fluorescence-based FRET approach after acceptor photobleaching. Yellow fluorescent protein (YFP) was fused to the N terminus of TAP/NXF1, and CFP was fused to the N terminus of ICP27. At 6 h after infection of transfected cells with 27-LacZ, cells were imaged using an argon laser to detect CFP emission at 458-nm excitation and YFP emission at 514-nm excitation. These images are labeled prebleach (Fig. 6). The bleaching of the acceptor protein YFP was performed using a 514-nm laser line at a specific location in the cell marked by the circles. The change in donor CFP fluorescence was quantified by comparing prebleach and postbleach images (Fig. 6). By this protocol, FRET is detected if donor fluorescence increases significantly more than that detected in negative controls. In the positive control in which CFP and YFP were both fused to ICP27, an intramolecular interaction occurred, and donor fluorescence increased significantly (Fig. 6A). However, there was no discernable increase in donor florescence with CFP-ICP27 and YFP-TAP/NXF1 (Fig. 6B). This was also the case when the CFP tag was placed on the C terminus of ICP27 (data not shown).

Because BiFC showed that these two proteins interact on a nanometer scale, we reasoned that ICP27 might interact with TAP/NXF1 when its N and C termini are interacting, and the simultaneous interaction of the N and C termini of ICP27 with TAP/NXF1 may be too short-lived or not stable enough for detection by conventional FRET. Therefore, we used a BiFC-based FRET approach. The proposed interaction of TAP/NXF1 with the ICP27 N and C termini is shown schematically in Fig. 7. When the

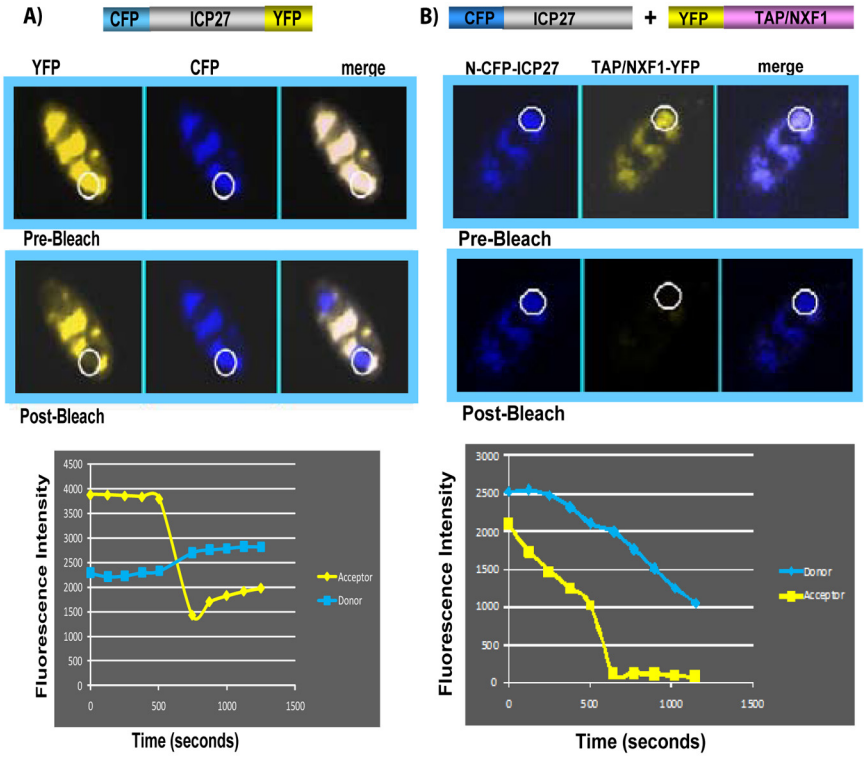

FIG 6 Interaction between CFP-ICP27 and YFP-TAP/NXF1 was not observed by FRET after acceptor photobleaching. (A) RSF were transfected with CFP-ICP27-YFP and were infected with 27-LacZ for 6 h. Merged images depicting the colocalization of YFP-ICP27 and CFP-ICP27 are shown, with the regions of interest for donor and acceptor images before and after bleaching circled. Quantification of FRET for the circled regions is displayed graphically as fluorescence intensity over time. (B) RSF were transfected with CFP-ICP27 and YFP-ICP27 and were then infected with 27-LacZ for 6 h. Merged images depicting the colocalization of CFP-ICP27 and YFP-TAP/NXF1 are shown, with the regions of interest for bleaching circled. Quantification of FRET for the circled regions is displayed graphically as fluorescence intensity over time, as described in Materials and Methods. FRET analysis was performed by using an LSM confocal microscope at a magnification of ×63.

N and C termini come together in NC-Venus-ICP27 and Venus refolds so that fluorescence occurs, ICP27 becomes locked in this configuration because Venus renaturation occurs through covalent bonding (Fig. 7A). Thus, the N and C termini are held together in a fixed position, and both ends would be accessible for TAP/NXF1 binding. Interaction with CFP-TAP/NXF1 would result in fluorescence energy transfer to donor CFP before photobleaching of the Venus acceptor (Fig. 7B). If FRET occurred before photobleaching of the acceptor, then the donor fluorescence should increase after photobleaching, because there is no longer a flow of excited-state energy from the donor to the acceptor. This is in fact what occurred. We observed an increase in donor fluorescence after acceptor photobleaching (Fig. 7C). The interaction was functional because in vNC-Venus-ICP27-infected cells that were transfected with CFP-TAP/NXF1, the infected cell expressing CFP-TAP/NXF1 showed that NC-Venus-ICP27 was exported to the cytoplasm (Fig. 7D).

Percent FRET was calculated from FRET efficiencies that were quantified by analysis of at least 30 bleached regions of interest for each FRET experiment, as described below in Materials and Methods. This is shown graphically in Fig. 8 for NC-Venus-ICP27 and CFP-TAP/NXF1 at 6 and 8 hours after infection, respectively (middle). CFP-ICP27-YFP, which served as the positive control, is shown at 6 and 8 hours after infection (Fig. 8, top). FRET was not detected for CFP-ICP27 and ICP27-YFP, as we reported previously (27), because ICP27 head-to-tail intermolecular interaction does not occur and thus served as a negative control (Fig. 8, bottom left). FRET was also not detected between CFP-ICP27 and YFP-TAP/NXF1 (Fig. 8, bottom right). We conclude that TAP/NXF1 interacts with both the N and C termini of ICP27, which are in an intramolecular head-to-tail association.

DISCUSSION

The initial goal of this study was to determine if we could demonstrate direct interaction *in vivo* between ICP27 and TAP/NXF1 and between ICP27 and Hsc70, as both of which colocalize and coimmunoprecipitate with ICP27. We used fluorescence-based approaches and showed that both TAP/NXF1 and Hsc70 interact directly *in vivo* and that ICP27's C-terminal zinc finger must be intact for functional interaction. This was also the case for head-to-tail association of ICP27, as shown previously (27). We further determined that interaction with TAP/NXF1 is dependent upon head-to-tail intramolecular interaction of ICP27. This was demonstrated using BiFC-based FRET in which the N and C termini of ICP27 are first required to undergo intramolecular interaction to allow Venus refolding before FRET can occur with CFP-TAP/NXF1. Although the percent FRET seen with CFP-TAP/NXF1 and NC-Venus-ICP27 was somewhat lower than that seen with NC-Venus-ICP27 alone (Fig. 8), this is likely because intramolecular interaction would be kinetically favored over intermolecular interaction.

Several cellular proteins have been shown to fold into a head-

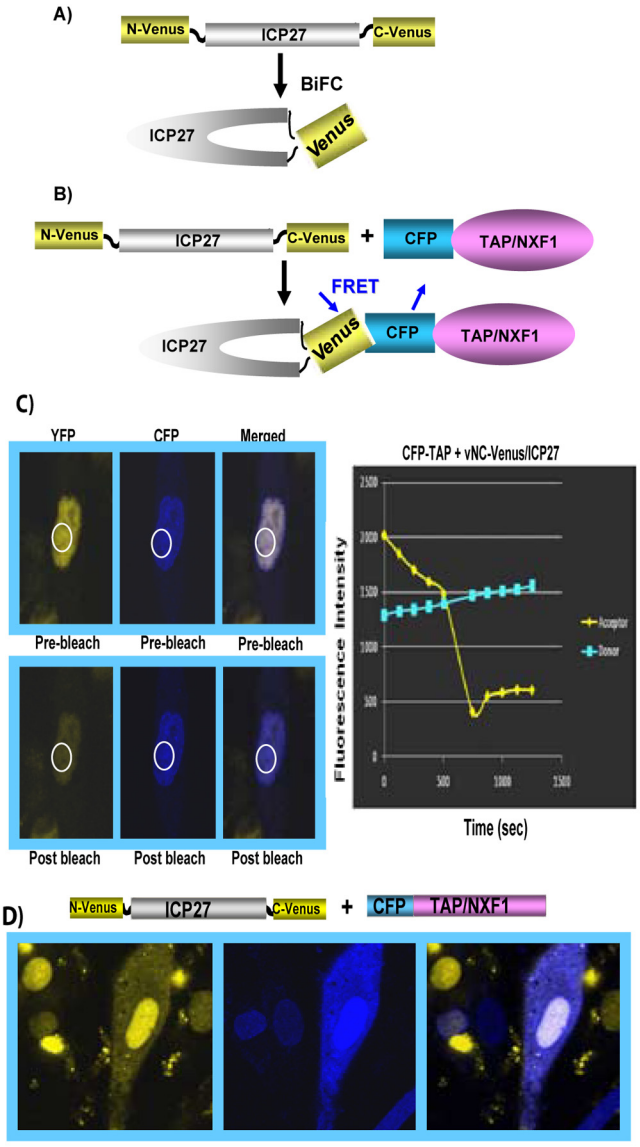

FIG 7 BiFC-FRET after photobleaching demonstrates the interaction of TAP/NXF1 with ICP27 upon head-to-tail association. (A) Schematic representation of BiFC for NC-Venus-ICP27. (B) Model showing FRET between CFP-TAP/NXF1 and NC-Venus-ICP27. (C) RSF were transfected with CFP-TAP/NXF1 and were subsequently infected with vNC-Venus-ICP27 at an MOI of 10. Merged images depicting the colocalization of ICP27 with TAP/NXF1 are shown, with the regions of interest circled before and after bleaching of the acceptor. Quantification of FRET for the circled regions is displayed graphically as fluorescence intensity over time. FRET analysis was performed as described in the legend to Fig. 6. (D) RSF were transfected with CFP-TAP/NXF1 and were subsequently infected with vNC-Venus-ICP27 for 6 h. Venus and CFP fluorescence were viewed directly using an LSM confocal microscope at a magnification of ×63.

to-tail conformation to regulate interactions with ligands or other proteins. For example, NHERF1/EBP50 folds in a head-to-tail conformation that inhibits the interaction of its PDZ domains with ligands (38). The scaffold protein PDZK1 undergoes a head-to-tail intramolecular interaction that negatively regulates its interaction with EBP50 (21). Zyxin, which is an adhesion protein, prevents binding to the vasodilator-stimulated phosphoprotein (VASP) through head-to-tail intramolecular interaction for regulation of actin assembly (19). The large cytoskeletal protein talin regulates its interaction with integrins, actin, and vinculin by undergoing intramolecular interaction through its N and C termini (22). Thus, ICP27 may regulate its interactions with proteins that interact with both its N and C termini through head-to-tail intramolecular association.

Nuclear magnetic resonance (NMR) structural analysis of the N-terminal 160-amino-acid region of ICP27, encompassing the leucine-rich region, the nuclear localization signal, the RGG box RNA binding domain and binding sites for TAP/NXF1 (3), Hsc70 (5), RNA polymerase II (12), RNA export factors Aly and Ref (4), and SR protein kinase (2), showed that it is highly flexible and appears to be intrinsically disordered (16, 39). Intrinsically, unfolded proteins have been found to undergo dynamic interactions of coupled binding and folding events (40). The large number of protein interactions that ICP27 undergoes are likely possible because of this flexibility in structure. We have reported that phosphorylation and arginine methylation regulate some of ICP27's protein interactions (16–18). Both of these modifications cause local structural changes, which may increase or decrease ICP27's affinity for a binding partner. Similarly, intramolecular association would also alter conformation, and the head-to-tail interaction may interchange between open and closed configurations, serving to regulate ICP27 interactions with some proteins. We have shown that the N-terminal leucine-rich region and the C-terminal zinc finger must be intact for intramolecular interaction (27), and here we showed that the zinc finger is required for functional interaction with TAP/NXF1 and Hsc70. Future studies will address what regulates the exchange between open and closed states in the intramolecular interaction.

MATERIALS AND METHODS

Cells, recombinant plasmids, and viruses. Rabbit skin fibroblasts (RSF) and Vero cells were grown on minimal essential medium supplemented with 10% fetal bovine serum. Plasmids pN-Venus-ICP27-C-Venus, pN-Venus-ICP27, pICP27-C-Venus, pN-CFP-ICP27-C-YFP, pN-CFP-ICP27, and pICP27-C-YFP were described previously (27). Plasmid pICP27-C483,488S was generated by site-directed mutagenesis of pSG130B/S, which carries the wild-type ICP27 gene (41), using a Stratagene QuikChange kit. Plasmid pICP27-C483,488S–C-Venus was created by site-directed mutagenesis of plasmid pICP27-C-Venus. Plasmid pICP27-C–CFP was constructed from plasmid pSG130B/S (41) by engineering an EcoRI site to disrupt the ICP27 stop codon at amino acid 512. CFP cDNA was ligated into the EcoRI site using EcoRI linkers. Plasmid pCFP-TAP/NXF1 was constructed by ligating TAP/NXF1 cDNA in frame into pEYFP-C1 (Clontech). To construct pN-Venus-TAP/NXF1, pCFP-TAP/NXF1 was digested with AgeI and BspI to release CFP. The ends were modified to create an EcoRI site, and sequences from the fluorescent protein Venus (35), corresponding to amino acids 1 to 154, were inserted into the EcoRI site. Plasmid pN-Venus-Hsc70 was similarly constructed from pGFP-Hsc70 (5).

HSV-1 strain KOS, ICP27 mutants 27-LacZ (42) and 27-GFP (green fluorescent protein) (15), and vNC-Venus-ICP27 (27) were described previously. To construct recombinant viruses expressing ICP27-C–CFP and N-CFP–ICP27-C483,488S, Vero cells were cotransfected with the corresponding plasmid DNA encoding the CFP-ICP27 fusion proteins and HSV-1 viral DNA to allow homologous recombination. Cells were overlaid 48 h after transfection with 2% agarose in phosphate-buffered saline (PBS) and were monitored for cyan plaques. Five rounds of plaque purification were performed, and the correct insertions were confirmed by sequencing. Recombinant viruses were termed vICP27-C–CFP and vN-CFP–ICP27-C483,488S.

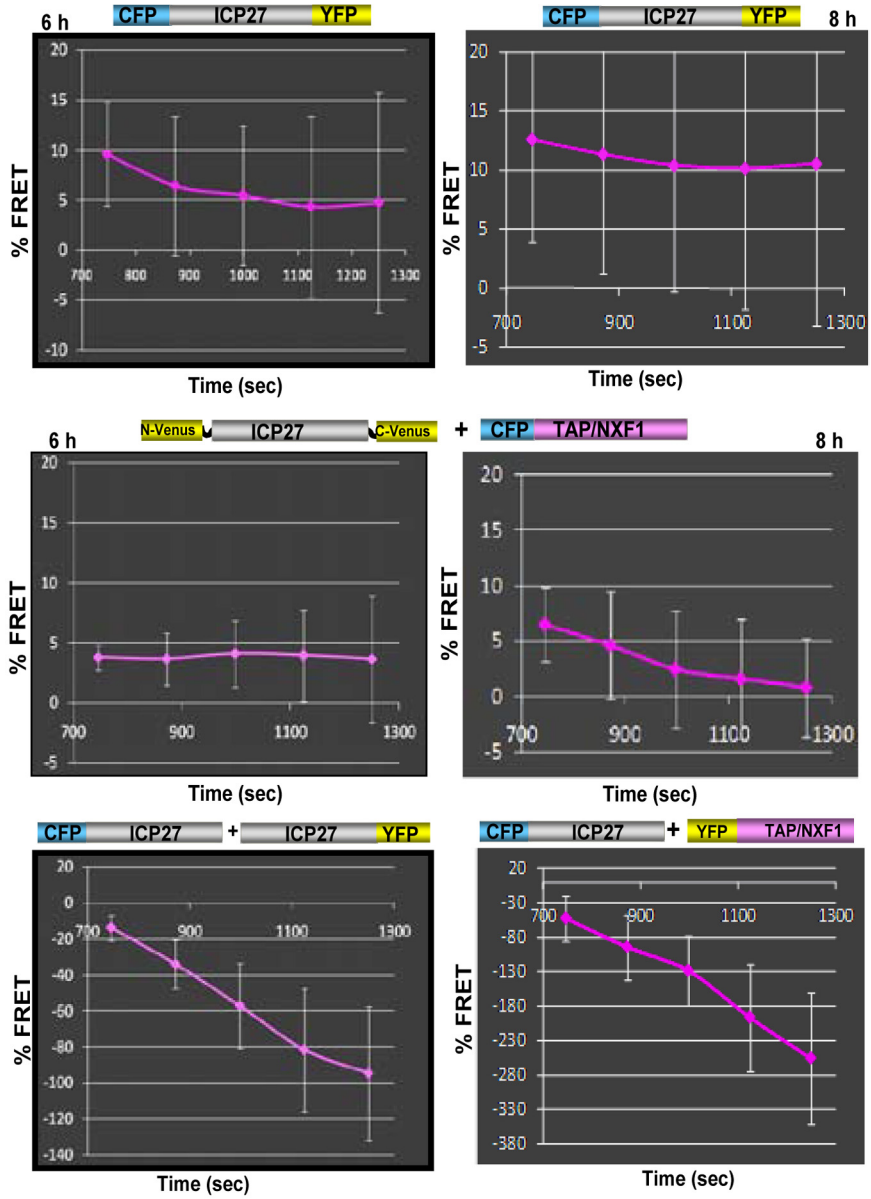

FIG 8 Analysis of percent FRET over time. RSF were transfected with the constructs indicated and were subsequently infected with 27-LacZ or with vNC-Venus-ICP27, as indicated. FRET after acceptor photobleaching was performed by photobleaching the acceptor protein Venus or YFP at a specific location within the cell using the 514-nm laser line at 100% transmission. The change in donor fluorescence was quantified by comparing prebleach and postbleach levels of CFP fluorescence from the images. The FRET efficiency (EF) obtained from at least 30 different bleached regions of interest was calculated as described in Materials and Methods. FRET efficiency is shown as percent FRET over time. Experiments were performed in triplicate. Error bars are shown.

One-step viral growth curves. Vero cells were infected with HSV-1 KOS, 27-GFP, vICP27-C–CFP, and vN-CFP–ICP27-C483S,C488S at a multiplicity of infection (MOI) of 1. Experiments were performed in triplicate, and virus was harvested at 0, 4, 8, 16, and 24 h after infection. Plaque assays were performed in duplicate with Vero cells.

Immunofluorescence. RSF grown on glass coverslips were transfected with plasmid DNA encoding wild-type ICP27 (pSG130B/S) or ICP27-C483S,C488S and with plasmid DNA encoding TAP/NXF1-GFP (3) using Lipofectamine 2000, and 18 h later, cells were infected with 27-LacZ at an MOI of 10 to induce expression of ICP27 constructs, which are under the control of their native promoters, by VP16. Cells were fixed at 8 h after infection with 3.7% formaldehyde and were stained as described previously (5) with anti-ICP27 monoclonal antibody (P1119; Virusys). GFP fluorescence was visualized directly. For infections with vICP27-C–CFP and vN-CFP–ICP27-C483,488S, RSF were infected with each virus at an MOI of 10. Cells were fixed at 4 and 10 h after infection, and CFP fluorescence was visualized directly using a Zeiss LSM 510 Meta confocal microscope at a magnification of ×63.

BiFC. BiFC analysis was performed in transient transfection assays as described previously (27). RSF were either transfected with N-Venus/ICP27/C-Venus plasmid DNA or were cotransfected with N-Venus–TAP/NXF1 and ICP27/C-Venus; N-Venus–TAP/NXF1 and ICP27-C483,488S–C-Venus; N-Venus–Hsc70 and ICP27–C-Venus; or N-Venus–Hsc70 and ICP27-C483,488S–C-Venus in glass-bottom culture dishes (MatTek Corporation) using Lipofectamine 2000. Eighteen hours after transfection, cells were infected with 27-LacZ at an MOI of 10.

Cells were viewed directly for Venus fluorescence using a Zeiss LSM 510 Meta confocal microscope at a magnification of ×20 to view fields of cells and at a magnification of ×63 to observe intracellular details. BiFC images were always taken with the same acquisition settings. The gain and offset were always exactly the same for the 514-nm laser line. The settings were determined by the positive control first, so that the images are not too bright, and all subsequent images were taken with the same settings. Images were taken directly, and the brightness/contrast was not changed after the image was taken.

FRET by acceptor photobleaching. Plasmid DNA encoding N-CFP–ICP27-C–YFP or N-YFP–TAP/NXF1 was transfected into RSF grown on glass-bottom dishes. Cells transfected with N-CFP–ICP27-C–YFP were infected with 27-LacZ. Cells transfected with N-YFP–TAP/NXF1 were infected with vN-CFP–ICP27. CFP-YFP FRET by acceptor photobleaching was performed at 8 h after infection using an LSM 510 Meta confocal microscope to detect emission from CFP, excited at 458 nm, and YFP, which was excited at 514 nm, as described previously (30). In this procedure, the acceptor protein, YFP, was photobleached at a specific location within the cell using the 514-nm laser line. The change in donor fluorescence was quantified by comparing prebleach and postbleach images. The FRET efficiency (EF) from at least 30 different bleached regions of interest was calculated using the following formula:

$$EF = (I_{postbleach} - I_{prebleach})/I_{postbleach}$$

where "*I*" is the average CFP fluorescence intensity after background subtraction. Using the LSM 510 Meta software, the average fluorescence intensities of the background (area outside the cell) for the acceptor and donor were measured, and these values were subtracted from average intensities in the regions of interest before and after bleaching

For BiFC-based FRET after photobleaching, RSF were transfected with N-CFP–TAP/NXF1 for 18 h and were then infected with vN-Venus/ICP27/C-Venus (27) at an MOI of 10. CFP-Venus FRET after acceptor photobleaching was performed by photobleaching the acceptor protein Venus at a specific location within the cell using the 514-nm laser line at 100% transmission. The change in donor fluorescence was quantified by comparing prebleach and postbleach levels of CFP fluorescence from the images. The FRET efficiency (EF) from at least 30 different bleached regions of interest was calculated as described above. FRET efficiency is shown as percent FRET over time in Fig. 8. Experiments were performed in triplicate.

Western blot analysis. RSF were transfected with pN-Venus-ICP27-C-Venus or pSG130B/S or were cotransfected with pN-Venus-TAP/NXF1 and pICP27-C-Venus or with pN-Venus-TAP/NXF1 and pICP27-C483,488S-C-Venus. Cells either were mock infected or were infected with 27-LacZ for 8 h. Infected cell monolayers were harvested by scraping the cells into 2× electrophoresis sample solution (12). Proteins were fractionated on a 10% sodium dodecyl sulfate (SDS)-polyacrylamide gel and transferred to nitrocellulose. Membranes were probed with antibodies against GFP (Clontech Living Colors), ICP27, and β-actin (Sigma-Aldrich), as described previously (27).

ACKNOWLEDGMENTS

This work was supported by National Institute of Allergy and Infectious Diseases grants AI61397 and AI21515.

REFERENCES

1. **Bryant, H. E., S. Wadd, A. I. Lamond, S. J. Silverstein, and J. B. Clements.** 2001. Herpes simplex virus IE63 (ICP27) protein interacts with spliceosome-associated protein 145 and inhibits splicing prior to the first catalytic step. J. Virol. **75**:4376–4385.
2. **Sciabica, K. S., Q. J. Dai, and R. M. Sandri-Goldin.** 2003. ICP27 interacts with SRPK1 to mediate HSV-1 inhibition of pre-mRNA splicing by altering SR protein phosphorylation. EMBO J. **22**:1608–1619.
3. **Chen, I. B., L. Li, L. Silva, and R. M. Sandri-Goldin.** 2005. ICP27 recruits Aly/REF but not TAP/NXF1 to herpes simplex virus type 1 transcription sites although TAP/NXF1 is required for ICP27 export. J. Virol. **79**:3949–3961.
4. **Chen, I. B., K. S. Sciabica, and R. M. Sandri-Goldin.** 2002. ICP27 interacts with the export factor Aly/REF to direct herpes simplex virus 1 intronless RNAs to the TAP export pathway. J. Virol. **76**:12877–12889.
5. **Li, L., L. A. Johnson, J. Q. Dai-Ju, and R. M. Sandri-Goldin.** 2008. Hsc70 focus formation at the periphery of HSV-1 transcription sites requires ICP27. PLoS One **3**:e1491.
6. **Johnson, K. E., B. Song, and D. M. Knipe.** 2008. Role for herpes simplex virus 1 ICP27 in the inhibition of type I interferon signaling. Virology **374**:487–494.
7. **Aubert, M., and J. A. Blaho.** 1999. The herpes simplex virus type 1 protein ICP27 is required for the prevention of apoptosis in infected human cells. J. Virol. **73**:2803–2813.
8. **Gillis, P. A., L. H. Okagaki, and S. A. Rice.** 2009. Herpes simplex virus type 1 ICP27 induces p38 mitogen-activated protein kinase signaling and apoptosis in HeLa cells. J. Virol. **83**:1767–1777.
9. **Dobrikova, E., M. Shveygert, R. Walters, and M. Gromeier.** 2010. Herpes simplex virus proteins ICP27 and UL47 associate with polyadenylate-binding protein and control its subcellular distribution. J. Virol. **84**:270–279.
10. **Fontaine-Rodriquez, E. C., T. J. Taylor, M. Olesky, and D. M. Knipe.** 2004. Proteomics of herpes simplex virus infected cell protein 27: association with translation initiation factors. Virology **330**:487–492.
11. **Sandri-Goldin, R. M.** 2008. The many roles of the regulatory protein ICP27 during herpes simplex virus infection. Front. Biosci. **13**:5241–5256.
12. **Dai-Ju, J. Q., L. Li, L. A. Johnson, and R. M. Sandri-Goldin.** 2006. ICP27 interacts with the C-terminal domain of RNA polymerase II and facilitates its recruitment to herpes simplex virus-1 transcription sites, where it undergoes proteasomal degradation during infection. J. Virol. **80**:3567–3581.
13. **Zhi, Y., and R. M. Sandri-Goldin.** 1999. Analysis of the phosphorylation sites of the herpes simplex virus type 1 regulatory protein ICP27. J. Virol. **73**:3246–3257.
14. **Mears, W. E., and S. A. Rice.** 1996. The RGG box motif of the herpes simplex virus ICP27 protein mediates an RNA-binding activity and determines in vivo methylation. J. Virol. **70**:7445–7453.
15. **Souki, S. K., P. D. Gershon, and R. M. Sandri-Goldin.** 2009. Arginine methylation of the ICP27 RGG box regulates ICP27 export and is required for efficient herpes simplex virus 1 replication. J. Virol. **83**:5309–5320.
16. **Corbin-Lickfett, K., S. Rojas, L. Li, M. J. Cocco, and R. M. Sandri-Goldin.** 2010. ICP27 phosphorylation site mutants display altered functional interactions with cellular export factors Aly/REF and TAP/NXF1 but are able to bind herpes simplex virus 1 RNA. J. Virol. **84**:2212–2222.
17. **Rojas, S., K. Corbin-Lickfett, L. Escudero-Paunetto, and R. M. Sandri-Goldin.** 2010. ICP27 phosphorylation site mutants are defective in herpes simplex virus 1 replication and gene expression. J. Virol. **84**:2200–2211.
18. **Souki, S. K., and R. M. Sandri-Goldin.** 2009. Arginine methylation of the ICP27 RGG box regulates the functional interactions of ICP27 with SRPK1 and Aly/REF during herpes simplex virus 1 infection. J. Virol. **83**:8970–8975.
19. **Moody, J. D., J. Grange, M. P. Ascione, D. Booth, E. Bushnell, and M. D. Hansen.** 2009. A zyxin head to tail interaction regulates zyxin-VASP complex formation. Biochem. Biophys. Res. Commun. **378**:625–628.
20. **Umeki, N., H. S. Jung, S. Watanabe, T. Sakai, X. Li, R. Ikebe, R. Craig, and M. Ikebe.** 2009. The tail binds to the head-neck domain, inhibiting ATPase activity of myosin VIIA. Proc. Natl. Acad. Sci. U. S. A. **106**:8483–8488.
21. **LaLonde, D. P., and A. Bretscher.** 2009. The scaffold protein PDZK1 undergoes a head to tail intramolecular association that negatively regulates its interaction with EBP50. Biochemistry **48**:2261–2271.
22. **Roberts, G. C. K., and D. R. Critchley.** 2009. Structural and biophysical properties of the integrin-associated cytoskeletal protein talin. Biophys. Rev. **1**:61–69.
23. **Dietrich, K. A., C. V. Sindelar, P. D. Brewer, K. H. Downing, C. R. Cremo, and S. A. Rice.** 2008. The kinesin-1 motor protein is regulated by a direct interaction of its head and tail. Proc. Natl. Acad. Sci. U. S. A. **105**:8938–8943.
24. **Wong, Y. L., K. A. Dietrich, N. Naber, R. Cooke, and S. A. Rice.** 2009. The kinesin-1 tail conformationally restricts the nucleotide pocket. Biophys. J. **96**:2799–2807.
25. **Chong, H., and K. Guan.** 2003. Regulation of Raf through phosphorylation and N terminus-C terminus interaction. J. Biol. Chem. **218**:36269–36276.

26. **Fusco, D., C. Forghieri, and G. Campadelli-Fiume.** 2005. The pro-fusion domain of herpes simplex virus glycoprotein D (gD) interacts with the gD N terminus and is displaced by soluble forms of viral receptors. Proc. Natl. Acad. Sci. U. S. A. **102**:9323–9328.
27. **Hernandez, F. P., and R. M. Sandri-Goldin.** 2010. Herpes simplex virus 1 regulatory protein ICP27 undergoes a head-to-tail intramolecular interaction. J. Virol. **84**:4124–4135.
28. **Hu, C. D., Y. Chinenov, and T. K. Kerppola.** 2002. Visualization of interactions among bZIP and Rel family proteins in living cells using bimolecular fluorescence complementation. Mol. Cell **9**:796–798.
29. **Kerppola, T. K.** 2006. Visualization of molecular interactions by fluorescence complementation. Nat. Rev. Mol. Cell Biol. **7**:449–456.
30. **Karpova, T., and J. G. McNally.** 2006. Detecting protein-protein interactions with CFP-YFP FRET by acceptor photobleaching. Curr. Protoc. Cytom. Chapter 12:Unit12.7.
31. **Johnson, L. A., L. Li, and R. M. Sandri-Goldin.** 2009. The cellular RNA export receptor TAP/NXF1 is required for ICP27-mediated export of herpes simplex virus 1 RNA, whereas, the TREX-complex adaptor protein Aly/REF appears to be dispensable. J. Virol. **83**:6335–6346.
32. **Johnson, L. A., and R. M. Sandri-Goldin.** 2009. Efficient nuclear export of herpes simplex virus 1 transcripts requires both RNA binding by ICP27 and ICP27 interaction with TAP/NXF1. J. Virol. **83**:1184–1192.
33. **Burch, A. D., and S. K. Weller.** 2004. Nuclear sequestration of cellular chaperone and proteasomal machinery during herpes simplex virus type 1 infection. J. Virol. **78**:7175–7185.
34. **Livingston, C. M., M. F. Ifrim, A. E. Cowan, and S. K. Weller.** 2009. Virus-induced chaperone-enriched (VICE) domains function as nuclear protein quality control centers during HSV-1 infection. PLoS Pathog. **5**:e1000619.
35. **Nagai, T., K. Ibata, E. S. Park, M. Kubota, K. Mikoshiba, and A. Miyawaki.** 2002. A variant of yellow fluorescent protein with fast and efficient maturation for cell-biological applications. Nat. Biotechnol. **20**: 87–90.
36. **Kerppola, T. K.** 2008. Bimolecular fluorescence complementation: visualization of molecular interactions in living cells. Methods Cell Biol. **85**: 431–470.
37. **Kerppola, T. K.** 2009. Visualization of molecular interactions using bimolecular fluorescence complementation analysis: characteristics of protein fragment complementation. Chem. Soc. Rev. **38**:2876–2886.
38. **Morales, F. C., Y. Takahashi, S. Momin, H. Adams, X. Chen, and M. Georgescu.** 2007. NHERF1/EBP50 head to tail intramolecular interaction masks association with PDZ domain ligands. Mol. Cell. Biol. **27**: 2527–2537.
39. **Corbin-Lickfett, K., S. K. Souki, M. J. Cocco, and R. M. Sandri-Goldin.** 2010. Three arginine residues within the RGG box are crucial for ICP27 binding to herpes simplex virus 1 GC-rich sequences and for efficient viral RNA export. J. Virol. **84**:6367–6376.
40. **Dyson, H. J., and P. E. Wright.** 2005. Intrinsically unstructured proteins and their functions. Nat. Rev. Mol. Cell Biol. **6**:197–208.
41. **Sekulovich, R. E., K. Leary, and R. M. Sandri-Goldin.** 1988. The herpes simplex virus type 1 alpha protein ICP27 can act as a trans-repressor or a trans-activator in combination with ICP4 and ICP0. J. Virol. **62**: 4510–4522.
42. **Smith, I. L., M. A. Hardwicke, and R. M. Sandri-Goldin.** 1992. Evidence that the herpes simplex virus immediate early protein ICP27 acts post-transcriptionally during infection to regulate gene expression. Virology **186**:74–86.